Numerical Simulation of JCO-E Pipe Manufacturing Process and Its Effect on the External Pressure Capacity of the Pipe

NUMERICAL SIMULATION OF JCO-E PIPE MANUFACTURING PROCESS AND ITS EFFECT ON THE EXTERNAL PRESSURE CAPACITY OF THE PIPE[1]

Konstantinos Antoniou [a], Giannoula Chatzopoulou [a], Spyros A. Karamanos[2] [a,b], Athanasios Tazedakis [c], Christos Palagas [c], Efthimios Dourdounis [c]

[a] *Department of Mechanical Engineering, University of Thessaly, Volos, Greece*

[b] *School of Engineering, The University of Edinburgh, Scotland, UK*

[c] *Corinth Pipe Works S. A., Thisvi, Greece*

ABSTRACT

Large-diameter thick-walled steel pipes during their installation in deep-water are subjected to external pressure, which may trigger structural instability due to pipe ovalization, with detrimental effects. The resistance of offshore pipes against this instability is affected by local geometric deviations and residual stresses, introduced by the line pipe manufacturing process. In the present paper, the JCO-E pipe manufacturing process, a commonly adopted process for producing large-diameter pipes of significant thickness, is examined. The study examines the effect of JCO-E line pipe manufacturing process on the external pressure resistance of offshore pipes, candidates for deepwater applications using nonlinear finite element simulation tools. The cold bending induced by the JCO forming process as well as the subsequent welding and expansion (E) operations are simulated rigorously. Subsequently, the application of external pressure is modeled until structural instability (collapse) is detected. Both the JCO-E manufacturing process and the external pressure response of the pipe, are modelled using a two-dimensional generalized plane strain model, together with a coupled thermo-mechanical model for simulating the welding process.

1 INTRODUCTION

The "JCO-E" manufacturing process is an efficient method for manufacturing thick-walled steel line pipes for deep water pipeline applications. It consists of five sequential mechanical steps, shown schematically in Figure 1: (a) the crimping of the plate edges, (b) the J phase, where the plate is formed into a J-shape, (c) the C phase, where the deformed plate is pressed into a quasi-round shape, (d) O phase, where the deformed plate obtains a round shape, and subsequently both ends of the plate are welded, and (e), the expansion (E) phase where the pipe geometry is improved through a mechanical expander [1].

In contrast with the manufacturing process and mechanical response of the UOE pipe, which has been studied extensively, a rather limited number of publications exist on the JCO-E manufacturing process. Following, some important publications referred to UOE manufacturing process are mentioned. An initial study on the effects of the UOE process on the mechanical behavior has been reported by Kyriakides *et al.* [2] using a simple analytical model. It has been shown for the first time that the cold forming of line pipes has a significant effect in determining the level of residual stresses in a line pipe, and should be taken into consideration for the prediction of

[1] Also presented in early form at Offshore Mechanics & Offshore Engineering OMAE 2017 Conference, Trondheim Norway, and published in the companion conference paper. OMAE 2017-61540: *Numerical Simulation of JCO Pipe Forming Process and its Effect on the External Pressure Capacity of the Pipe.*

[2] Corresponding author: spyros.karamanos@ed.ac.uk

the ultimate external pressure and pressurized bending capacity. Similar conclusions have been reported in the experimental works [3], [4]. A finite element study has been reported on the effect of UOE cold bending process on the collapse pressure by Herynk *et al*. [5] who employed an advanced two-surface plasticity model using a cyclic-plasticity model with nonlinear kinematic hardening. Chatzopoulou *et al*. [6] examined the effect of UOE cold bending process on pipes subjected to combined loading, extending the work reported in [5]. Additional publications have been reported by Toscano *et al*. [7] on the ultimate pressure capacity of UOE pipes, using finite element models and more traditional plasticity models. As far as the JCO manufacturing process, some resent publications are referred following. Chandel *et al*. [8] simulated the JCO-E manufacturing process and concluded that the dimensions of the tools/dies at every station of line pipe forming play a critical role in forming a line pipe, whereas Gao *et al*. [9] examined numerically the effect of punch pressing on final geometry. Krishnan and Baker [10] examined both JCO-E and JCO-C manufacturing processes (the latter process consists of compressing instead of expanding a JCO pipe at the final step) and their effect on material properties of the formed pipe and on structural performance. The effect of a JCO-C pipe on material properties of the formed pipe and the collapse pressure was investigated also by Reichel *et al*. [11].

The present study simulates the JCO-E manufacturing process and the mechanical behavior of a thick-walled JCO-E line pipe, candidate for deep offshore pipeline applications, using a rigorous finite element model. In the present model, upon completion of the simulation of the manufacturing process, the analysis proceeds in simulating the mechanical behavior of the line pipe under external pressure following a concept also employed in [5], [6] so that the effects of manufacturing on structural performance are taken into account in a rigorous manner. Using the present simulation, initial geometrical deviations (out-of-roundness and variation of thickness around the pipe circumference), residual stresses and material anisotropy of the line pipe at the end of the JCO-E manufacturing process can be predicted rigorously. A novelty of the present work consists of the simulation of the welding process, using a thermo-mechanical analysis at the weld neighborhood so that the complete manufacturing process is simulated.

To model steel material behavior of the plate during cold bending process a cyclic plasticity material model is used, based on the von Mises plasticity formulation and the nonlinear kinematic hardening rule, introduced elsewhere [6], capable of modelling both the yield plateau at initial yielding and the Bauschinger effect upon reverse plastic loading. It is inserted into the finite element model using a material-user subroutine and calibrated through available experimental data on reverse cyclic uniaxial loading of the steel material. A parametric analysis is also conducted to examine the effect of expansion on the ultimate capacity of the pipe.

2 NUMERICAL MODELING

2.1 Finite element modeling

A two-dimensional model is developed in the general-purpose finite element program ABAQUS/standard. The model describes the cross-sectional deformation of the pipe under generalized plane strain conditions. This allows for simulating both the manufacturing process from the flat plate to the circular shape configuration of the pipe, restraining out-of-plane displacements, as well as the subsequent application of external pressure in a sequence of steps within a single model in order to examine the pressure capacity of the JCO-E pipe. In the present study, the thermal effect of welding process on the structural response is also examined. The area of pipe affected by the thermal load (weld metal and heat affected zone) is considered as a part of the entire pipe where a thermomechanical analysis is conducted. This part is denoted as “weld part” (Figure 2). The effect of the size of the weld part is also

examined in the present study. In particular, two different geometries of that area are chosen. The first geometry (weld part A) is similar to the shape of the weld metal and the corresponding heat affected zone, as shown in the metallography of Figure 2a, which refers to a 22.2mm thick pipe, provided by Corinth Pipeworks S. A.; the second geometry (weld part B) corresponds to a larger area that contains the weld, as depicted in Figure 2b. A kinematic constraint (tie) is applied in the interface between the weld part and the rest of the pipe, which does not allow separation and relative sliding during the entire JCO-E process.

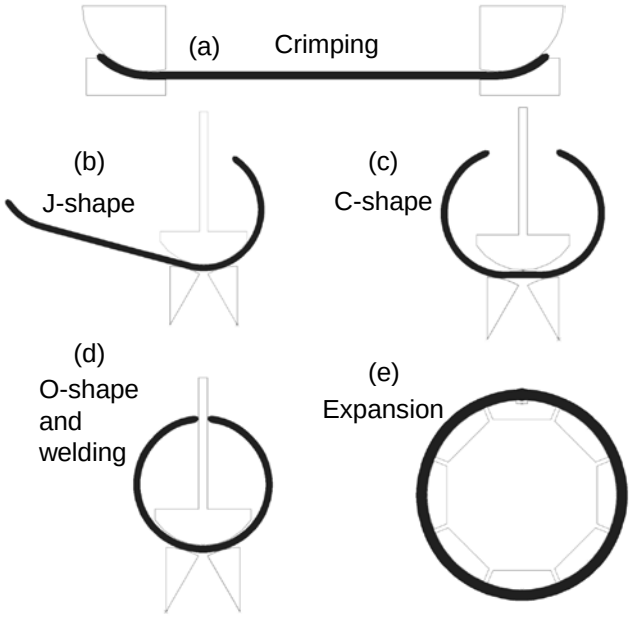

Figure 1: Schematic representation of the subsequent phases of JCO-E manufacturing process: (a) Crimping, (b) J-shape, (c) C-shape, (d) O-shape and welding, (e) Expansion.

The weld part is discretized using four-node, generalized plane strain thermally-coupled quadrilateral elements that assume, bilinear variation of displacement and temperature, denoted as CPEG4T in ABAQUS/Standard. The rest of the steel plate is discretized using four-node, reduced-integration generalized plane-strain continuum finite elements, denoted as CPEG4R in ABAQUS/standard. The forming dies are modeled as analytical rigid surfaces. The radius of curvature of the rigid parts for crimping and the subsequent punching steps is calculated according to expressions (1) below:

$$\begin{aligned} \varepsilon_{tot} &= \frac{t}{D_m} + \frac{\sigma}{E} \\ R_m &= \frac{t}{2\varepsilon_{tot}} \\ R_{in} &= R_m - \frac{t}{2} \\ R_{out} &= R_m + \frac{t}{2} \end{aligned} \qquad (1)$$

The geometric features of the plate and the forming tools are shown in Table 1. It is important to underline that the developed finite element model is capable of simulating both the manufacturing process and the subsequent application of external pressure,

considering an appropriate sequence of loading steps. Furthermore, a sensitivity analysis of collapse pressure to the number of elements through the thickness has been performed. This mesh convergence study concluded that 8 elements should be used through pipe wall thickness, and the size of elements around the circumference is equal to 6mm, which is 18.5% of pipe wall thickness.

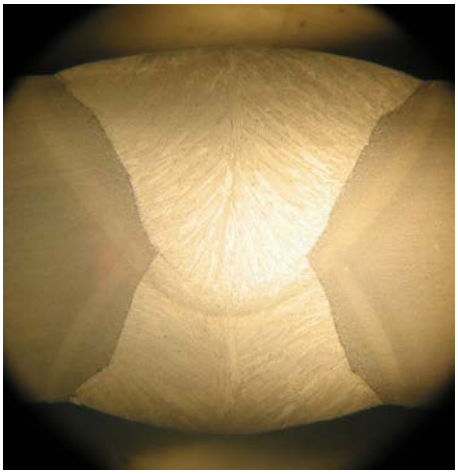

(a)

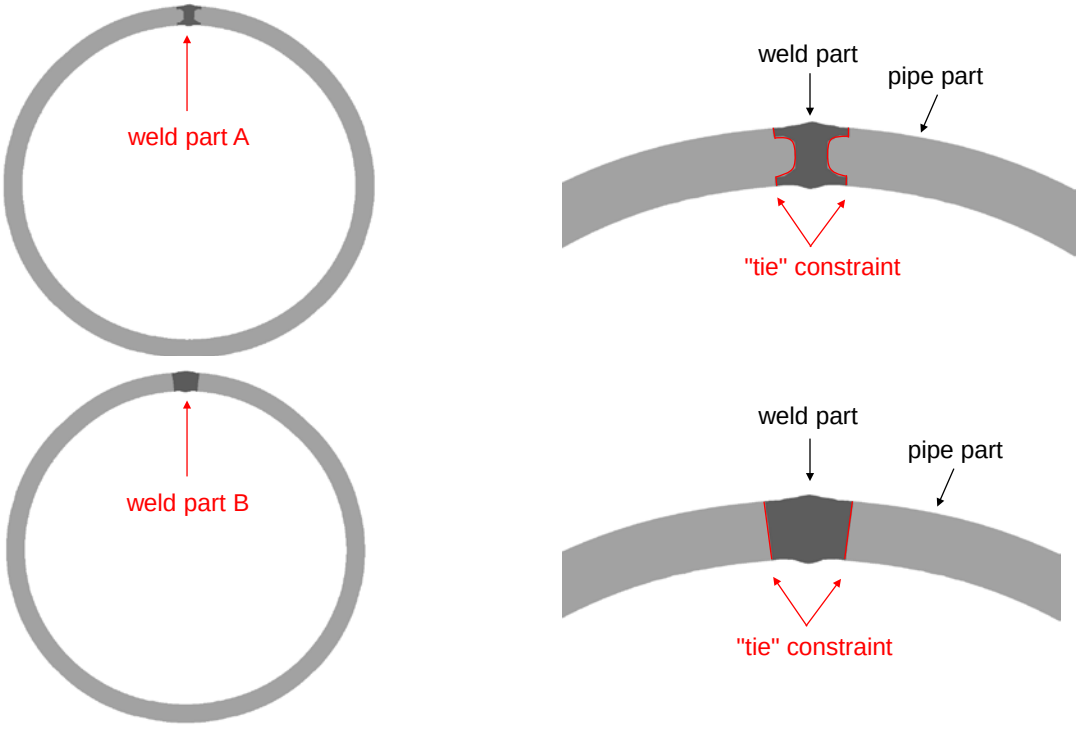

(b)

Figure 2: (a) Metallography of SAW weld of a 22.2mm thick X-70 line pipe provided by Corinth Pipeworks S.A.; (b) Schematic representation of the two different geometry configurations, used in the model for the weld part.

Table 1: Geometric parameters of the JCO-E manufacturing process for the 24-inch-diameter line pipe.

		Description	Value
Plate/Pipe	t	Plate thickness (mm)	32.33
	W	Plate width (mm)	1803
	σ_y	Steel yield stress (MPa)	498
	D	Pipe outer diameter (mm)	609.6
	D_m	$D_m=D-t$	577.27
Crimping	R_{in}	Internal crimping radius (mm)	265.4
	R_{out}	External crimping radius (mm)	259.53
JCO	R_{in}	Punch radius (mm)	259.53
Expansion		Mandrel radius (mm)	261
		Number of mandrel segments	8

2.2 Constitutive modeling

The accurate simulation of material behavior under reverse (cyclic) loading conditions is of major importance for modeling the JCO-E process and for the reliable prediction of line pipe capacity under external pressure. In the course of the JCO-E manufacturing process, the pipe material is deformed well into the plastic range and is subjected to reverse loading, characterized by the appearance of the Bauschinger effect. In the present study, a modified Armstrong-Frederick hardening model, described elsewhere [6], is used for simulating the steel plate material except for the weld part.

The material model is calibrated with a uniaxial stress-strain curve from uniaxial tensile testing of a steel coupon. In the present study, the material curve shown in Figure 3 is employed [5], [6]. The yield stress of steel material σ_y is equal to 498MPa (72ksi), corresponding to X-70 steel grade. The capability of the present material model in reproducing accurately the experimental uniaxial stress-strain curve of the X-70 steel is shown in Figure 3; both the “plateau” region upon initial yielding and the Bauschinger effect are described satisfactorily. It is noted that accurate description of the stress-strain curve in terms of the local rigidity of the steel material is important for variable prediction of steel line pipe resistance against external pressure collapse.

The material of the weld part is considered as steel material with yield stress equal to 550MPa (79ksi) which is 10.44% higher than the one of the base metal, so that an overmatching weld is represented. During the welding process, reverse loading in plastic region is occurred in weld part. For this purpose, a kinematic hardening model is used for the description of the material behavior. The temperature dependence on the mechanical properties used in this paper is presented in Table 2 and is similar to those reported in [12]. The dependence of stress-strain curve on temperature is shown in Figure 4. More details on the simulation of the weld part are offered in the next paragraph.

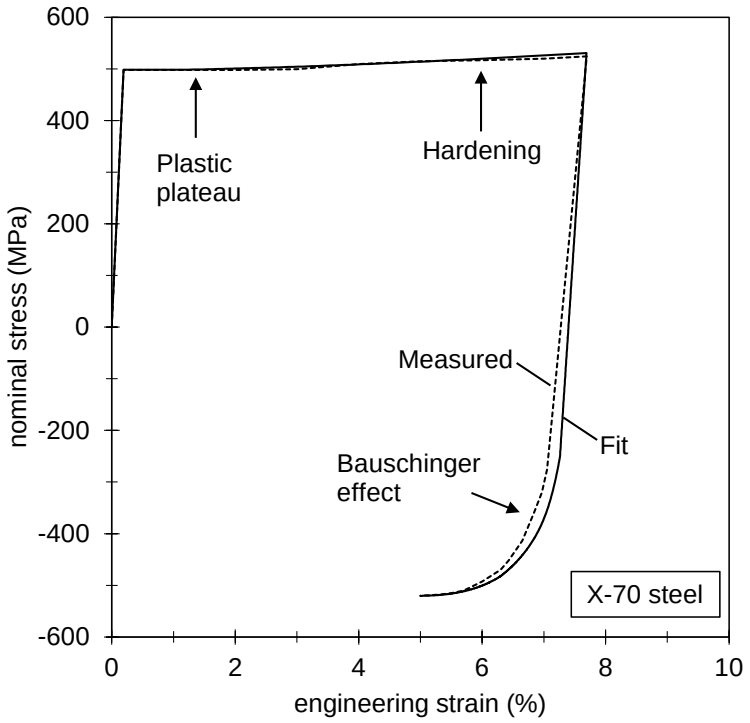

Figure 3: Test and material modeling for uniaxial X-70 stress-strain behavior [5].

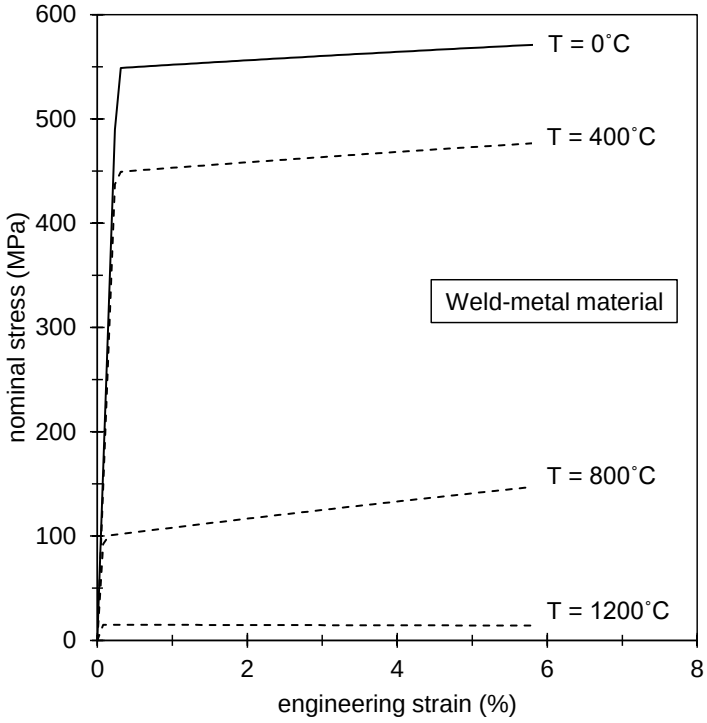

Figure 4: The dependence of stress-strain curve on temperature for the material of the weld part.

2.3 Finite element modeling of welding

A SAW welding process is employed consisting of two passes: (a) inside welding and (b) outside welding. The first pass employs an array of four electrodes, while the second employs an array of five electrodes, according to the welding procedure specification of Corinth Pipeworks S.A. The thermal load deposited on the surface of the pipe for each electrode is computed by multiplying the arc voltage with the arc current and the efficiency of the SAW welding process. A typical value of SAW efficiency is taken into account in the present analysis equal to 0.8, as suggested by Corinth Pipeworks S.A. The simulation of welding is carried out on a two-pass welding using a coupled thermo-mechanical analysis. More specifically, four steps are considered in the numerical model: (a) first pass (inside the pipe), (b) cooling of the first pass, (c) second pass (outside the pipe) and (d) cooling of the second pass. The thermal load induced into the weld area accounts for the mean value of the arc voltage and arc current from the multi-electrode array and is equal to 24.08 KW for the first pass and 25.49 KW for the second pass. In the present work, DFLUX subroutine is employed to impose the heat flux during each of the two passes. The distribution of heat flux implemented in the finite element model follows Goldak's ellipsoidal density distribution, as suggested in [13]. It is noted that the two-dimensional model, may not be possible to simulate heat flow in the longitudinal direction of the pipe, and therefore the present simulation assumes that heating of the steel material starts when the electrode is overhead. The variables of the thermal field associated with the present heat conduction analysis are: (a) the temperature, (b) the specific heat capacity, (c) the density, (d) the thermal conductivity. The dependence of specific heat, density and thermal conductivity on the level of temperature for weld part, considered in the present analysis, is shown in Table 2 and the values are similar to those reported in [12].

Table 2: Thermal and physical properties of weld part.

Temperature/ ^0C	Specific heat/ $\left(J \bullet kg^{-1} \bullet {}^0C^{-1}\right)$	Density/ $\left(g \bullet cm^{-3}\right)$	Thermal conductivity/ $\left(W \bullet m^{-1} \bullet {}^0C^{-1}\right)$	Poisson's ratio	Young's modulus/ GPa	Yield stress/ MPa
0	423	7.85	54.42	0.3	210	550
100	473	7.79	54.01	0.3	207	530
200	536	7.77	52.75	0.3	204	500
400	662	7.72	47.71	0.31	187.5	450
800	914	7.61	27.55	0.35	118.6	100
1200	1160	7.50	40.00	0.4	39.5	15

During the welding process, the temperature of the weld part of the model increases due to the thermal load input but heat is also lost due to natural convection and radiation. The heat flow densities for convection and radiation are taken into account in the present analysis by defining conduction and radiation contact surfaces around the weld part assuming an ambient temperature of 0˚C. During the O-phase, the two edges come together and appropriate kinematic constraints are employed, assuming perfect heat conduction between the two edges. Also, during thermal loading, appropriate kinematic constraints (similar to those applied in a real case in the pipe mill) are used in order to avoid any displacement of the cross-section; such a displacement would be undesirable during welding. The welding process is carried out using "death and birth" technique, which activates the elements corresponding to the filler material

in order to simulate the addition of new material in each pass. At the stage where the steel material melts (1200°C), the values of mechanical properties are considered very small so that material rigidity is minimized, as shown in the corresponding curve of Figure 4. Moreover, temperatures exceeding 1200°C will cause “stress-free annealing”, and to account for this effect one should effectively reset the accumulated plastic strain and, thereby, also the workhardening [13], [14]. In the finite element model, this stress-free annealing is implemented by setting the accumulated plastic strain equal to zero for a specific element if its temperature becomes equal or higher than 1200°C. Furthermore, when the material melts, convection will occur in the weld pool and in this case an increased value of thermal conductivity is used as shown in Table 2 [12].

3 NUMERICAL RESULTS FOR JCO-E MANUFACTURING PROCESS

During each stage of the manufacturing process, the plate is deformed in a different area in order to reach the final shape. In the first phase, the edges are crimped and all the other plate parts remain almost undeformed. After crimping, the J-phase follows in which one side of the plate is bent using a sequence of punching steps in order to obtain the J-shape. Afterwards, the plate is bent from the other side until it obtains a C shape. Subsequently, the punch presses the plate in the middle so that the plate obtains an O shape. Then, the welding process is carried out. Finally, expansion is performed using internal mandrels in order to improve the dimensional characteristics of the pipe. It is common practice in pipe mills that the expansion mandrel located at 12 o’ clock (top mandrel, weld location) may not be in contact with the pipe. The specific mandrel includes a groove of specific dimensions in order to minimize any effect on the weld zone during expansion (Figure 1e). The presence of this groove in the top mandrel has not been considered in the present finite element analysis. Figure 5, Figure 6 and Figure 7 depict the contour plots of the Von Mises stresses from the different stages of the simulation, indicating the areas which deform in every step of the process. In addition, the temperature field during the welding process is shown in Figure 6.

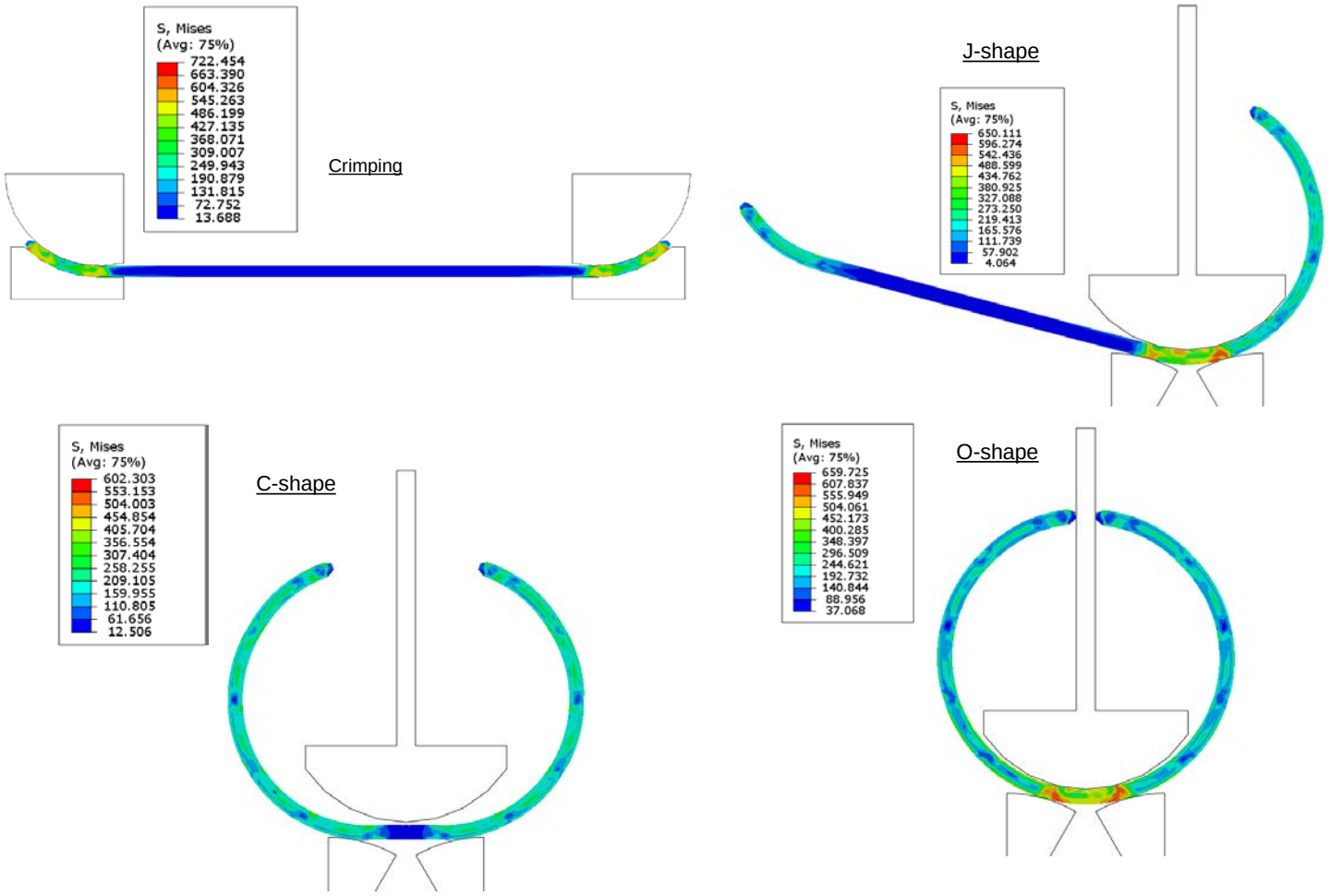

Figure 5: Numerical simulation of the crimping and JCO forming process; 9 punching steps.

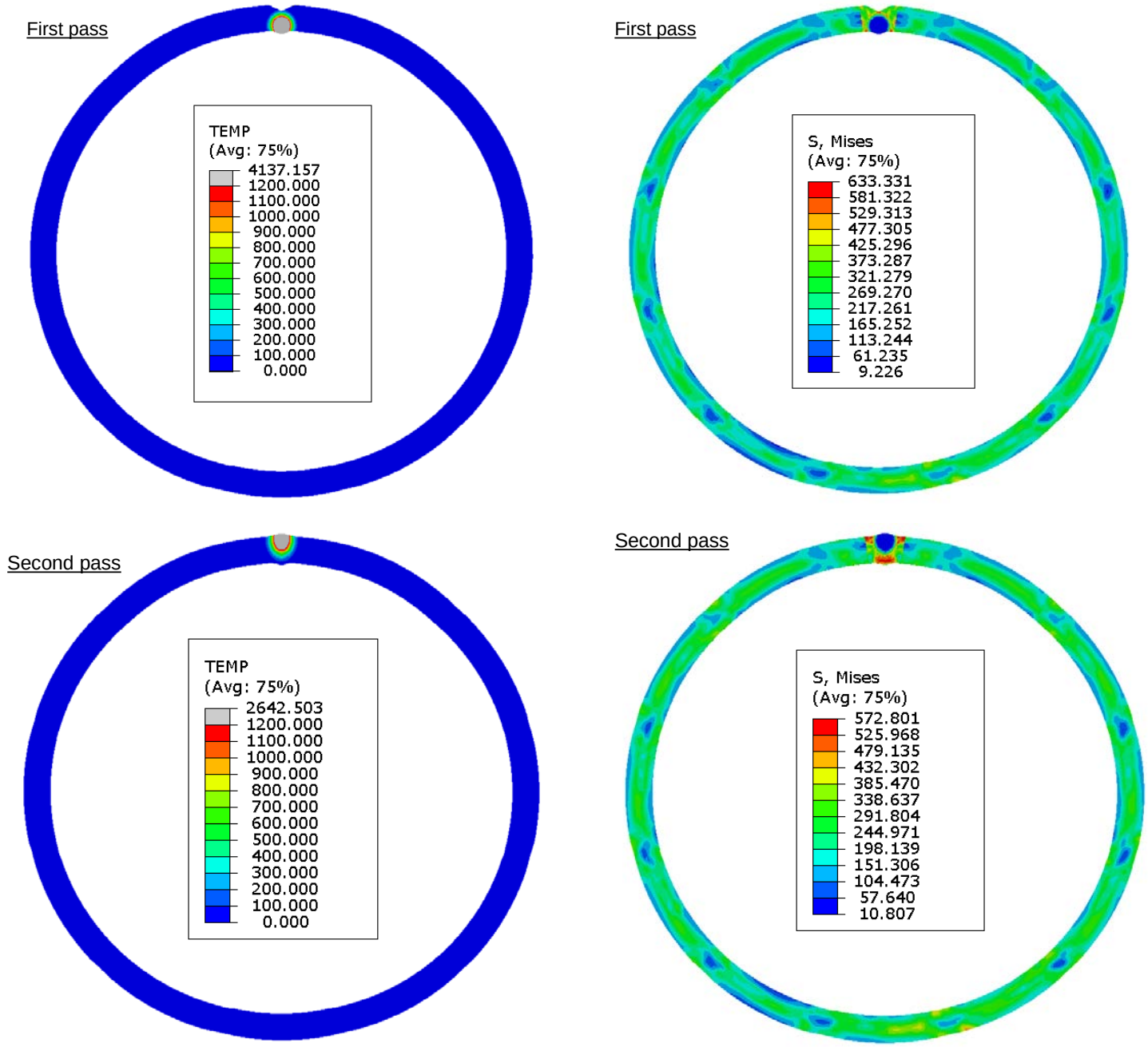

Figure 6: Distribution of temperature and Von Mises stress after the first and second welding pass; 9 punching steps.

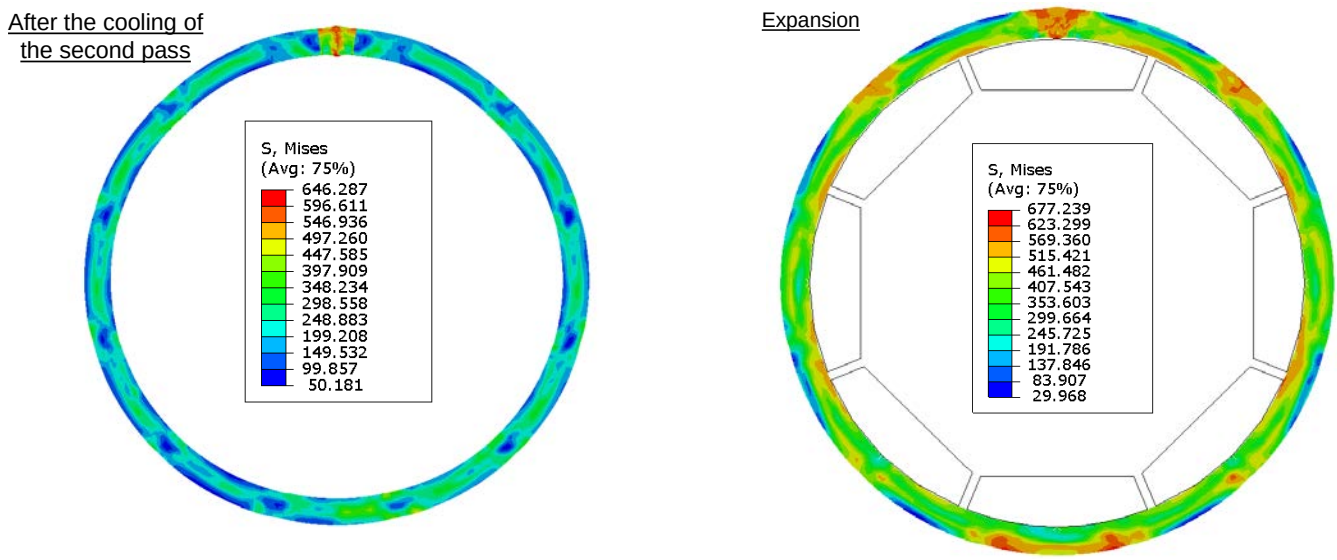

Figure 7: Numerical results for the Von Mises stress after cooling of the second pass and the expansion stage; 9 punching steps.

In the present study, a numerical analysis is conducted in order to examine the effect of the number of the punching steps and the effect of the size of the two different weld parts on the external pressure performance. Three cases are considered, with 9 steps, 15 steps, and 19 steps respectively. In addition, the value of the expansion displacement of the mandrel u_{E} constitutes a key parameter. In the present analysis, this displacement is considered equal to zero at the point where the first mandrel reaches contact with the inner surface of the pipe. It is noted that the line pipe with zero expansion $(u_{\mathrm{E}} = 0mm)$ is referred to as "JCO" case and will be used in the presentation of the results for comparison purposes. If the mandrels continue to more outwards beyond this stage, the circular plate is accommodating itself to the new mandrel position causing mainly bending deformation on the pipe wall. At the stage where all mandrel segments are in contact with the pipe walls, the pipe has reached a quasi-rounded shape and upon further outward displacement of the mandrels the pipe expands, increasing the length of its circumference and the pipe geometry is further improved. This is expressed by the so-called "expansion" hoop strain, denoted as ε_{E}, and defined by the following equation:

$$\varepsilon_{\mathrm{E}} = \frac{C_E - C_W}{C_W} \qquad (2)$$

where C_E and C_W are the mid-surface lengths of the pipe circumference after the expansion phase (and removal of the mandrels) and after unloading of the O-ing/welding step. A similar definition for the hoop expansion has also been suggested in [5] and [7]. Given the fact that the values of C_E are measured after the mandrels are removed, ε_{E} may be considered as a "permanent" expansion hoop strain, which accounts for the small "elastic rebound" at the end of the expansion. It should also be noted that this expansion hoop strain is quite different than the local hoop strain of the pipe material at a specific location after the manufacturing process; the value of ε_{E} should be considered as a "macroscopic" strain like parameter to quantify the expansion size. Figure 8 depicts the relation between the value of the expansion displacement u_{E} and the corresponding permanent expansion hoop strain ε_{E}. In the present analysis, the value of u_{E} ranges from $u_{\mathrm{E}} = 0mm$ (corresponding to the "no expansion" JCO case) to $u_{\mathrm{E}} = 9mm$. The maximum value of u_{E}

corresponds to a value of permanent expansion hoop strain ε_{E} equal to 0.85%, 1.01% and 0.83% for the cases of 9, 15, and 19 steps respectively. The results in Figure 8 show that the permanent expansion hoop strain ε_{E} is a non-linear function of the expansion displacement u_{E}. More specific, at the beginning the slope of the line (Figure 8) is almost zero. This is attributed to the fact that not all mandrels have been in contact with the inner surface of the pipe. Then, as the mandrels move, the shape of the cross-section of the pipe becomes rounded and the slope is gradually increased. Finally, for larger values of displacement of mandrels, the pipe has a circular shape, all mandrels are in contact and, as a result, the slope of the curve obtains a constant value. The analytical expression for slope of the $\varepsilon_{\mathrm{E}} - u_{\mathrm{E}}$ curve can be calculated according to expression (3) below, which is directly obtained from equation (2) assuming axisymmetric geometry of line pipe cross-section during expansion. One can readily verify that the value of slope ($\Delta\varepsilon_E / \Delta u_E$) at the final part of the diagrams obtained from the finite element results is quite close to the one from equation (3).

$$\frac{\Delta\varepsilon_E}{\Delta u_E} = \frac{2}{D_m} \tag{3}$$

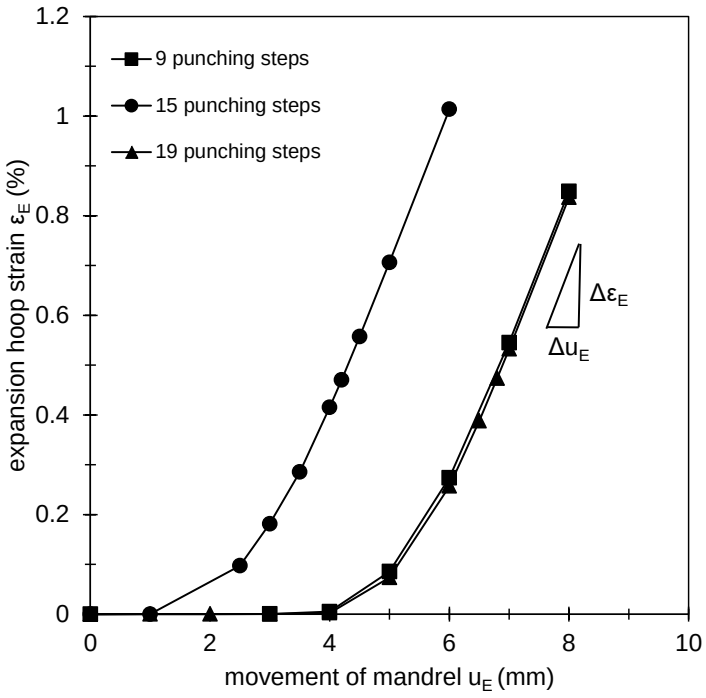

Figure 8: Variation of the induced (permanent) hoop expansion strain ε_E in terms of the expansion displacement value u_E of the formed JCO-E pipe.

3.1 Line pipe ovalization and out-of-roundness

An important parameter for assessing the mechanical behavior of offshore pipes subjected to external pressure is the residual ovalization of pipe cross-section after the manufacturing process, often referred to as "cross-sectional ovality". Initial ovalization is a geometric imperfection of the line pipe and has a significant effect on the ultimate capacity under external pressure [1], causing premature collapse with respect to the perfect pipe without initial ovalization. To quantify pipe cross-sectional ovality, the ovality parameter Δ is employed, defined as:

$$\Delta = \frac{|D_1 - D_2|}{D_1 + D_2} \tag{4}$$

where D_1 and D_2 are the maximum and minimum outer diameters of the pipe cross-section respectively, measured at the end of the JCO-E process. At the end of the manufacturing process, before pressure is applied, the value of Δ is denoted as Δ_0 and referred to "initial ovality", whereas, upon pressure application, the value of Δ increases.

The effect of expansion hoop strain ε_E on the value of the initial ovalization parameter Δ_0 is shown in Figure 9 for the three different cases. Before expansion is applied (ε_E = 0%), the ovalization corresponding to 15 punching steps is significantly lower than the other two cases (9 and 19 steps). For the case of 9 punching steps, the number of punches may not be adequate to develop a circular shape, and is associated with significant ovalization. When 15 punching steps are employed, pipe out-of-roundness improves, the shape after the O phase is symmetric (Figure 10a) and the ovalization is significantly smaller. However, exceeding this number of punches (e.g. 19 punches), there is overlapping of the areas influenced by adjacent punches. As a consequence, a non-symmetric pipe shape is obtained at the end of the O phase (Figure 10b), resulting in higher ovalization before expansion (ε_E = 0%). Upon application of expansion, ovality drops rapidly for the cases of 9 and 19 punches, as shown in Figure 9, and obtains quite small values (less than 0.2%) at ε_E = 0.3%. For the case of 15 punching steps, the ovalization before expansion (ε_E = 0%) is quite low compared to the other two cases, and remains below 0.1% for the entire range of ε_E values examined. Based on those results, a number of 15 punching steps appears to be optimum for the pipe under consideration.

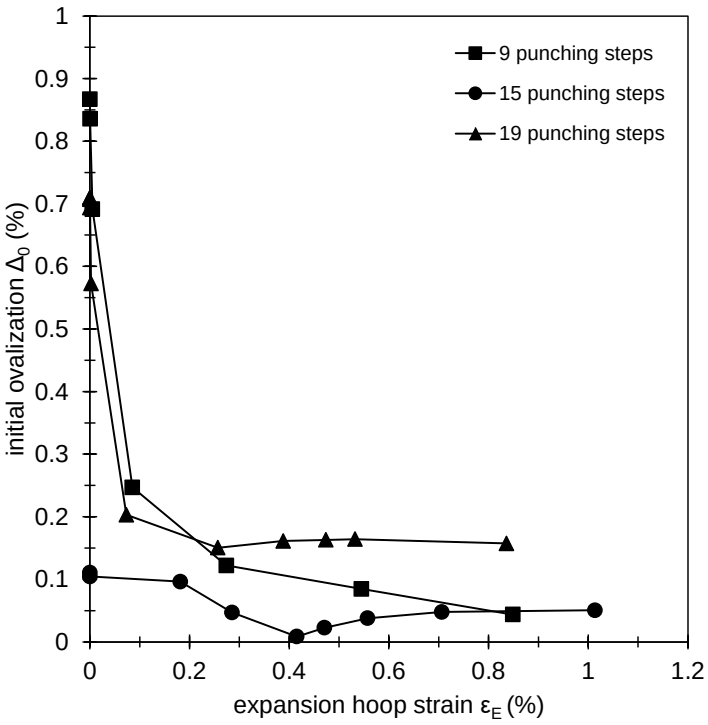

Figure 9: Ovality parameter in terms of permanent expansion hoop strain.

Figure 10: Deformed plate at the end of the C and O phase; (a) 15 punching steps; (b) 19 punching steps.

3.2 Pipe Thickness

Due to manufacturing process, the thickness of a JCO-E pipe after forming is somewhat different than the thickness of the initial steel plate. The average thickness of the pipe $t_{average}$ around the cross-section is computed at the end of the JCO-E process (including unloading) and the results are shown in Figure 11 with respect to the expansion hoop strain ε_E. The plot presents the results from the case with 9 punching steps and indicates that the mean thickness of the formed pipe, measured at 3 o'clock, 6 o'clock and 9 o'clock position, decreases with increasing values of hoop expansion in a quasi-linear manner. The average thickness for a pipe with zero expansion $\varepsilon_E = 0\%$, corresponding to the "JCO" case, is equal to 32.15mm, very close to the nominal plate thickness. This reduction is mainly due to the punching steps of the steel plate. For $\varepsilon_E = 0.84\%$ the average thickness reduces to 32.08mm, corresponding to a 0.77% thickness reduction with respect to the initial plate thickness, which is mainly due to circumferential expansion.

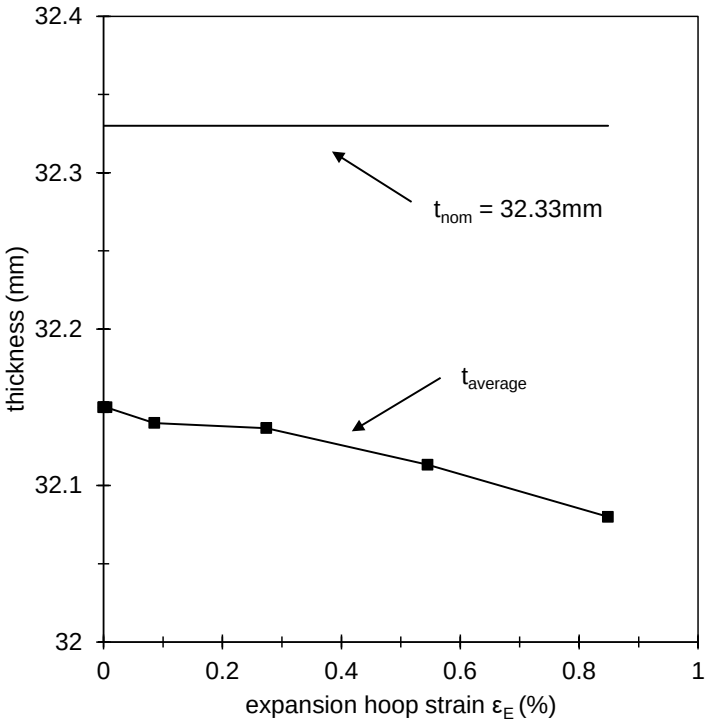

Figure 11: Effect of the expansion hoop strain ε_E on the average thickness $t_{average}$ of the JCO pipe.

3.3 Line Pipe Material properties

The structural performance of the line pipe depends strongly on its material mechanical properties. The JCO-E forming process introduces significant stresses and deformations, strain hardening region is appeared and, consequently, the stress-strain response of the line pipe is modified with respect to the plate material. In particular, material anisotropy and non-homogeneity may have a significant effect on the mechanical behavior of offshore pipes. Anisotropy means that the yield stress in the axial direction is different than the yield stress in the hoop direction and non-homogeneity means that the yield stress in the hoop direction at the internal (intrados) and external (extrados) surface of the pipe is different. In practice, the mechanical properties of the line pipe steel material at the end of the JCO-E forming process are evaluated by extracting two strip specimens from the extrados and the intrados in the hoop direction of the pipe to examine the response in two areas. Furthermore, two specimens are obtained from the longitudinal and the hoop direction of the pipe, in order to examine material anisotropy in the two principal directions at the external surface of the pipe. These strip specimens are subjected to uniaxial loading, so that the corresponding stress-strain curves are obtained [1].

A numerical simulation of the above testing procedure is attempted in the present study for the case of 9 punching steps. More specifically, a circumferential location 90º away from the weld region (3 o'clock) is selected in the numerical model. Two integration points are selected at this location, one at the external surface of the pipe and the other at the internal surface in order to examine (a) the compression response in the hoop direction at the intrados and extrados of the pipe and (b) the material anisotropy in the hoop and the axial direction. Throughout the simulation of the forming process, all material state parameters (stresses, strains) are recorded at those integration points. Subsequently, finite element model of a "unit cube" is considered and the material parameters from the selected integration point as computed at the end of manufacturing in the forming model are introduced as initial state variables in that model. First a step with zero external loading is performed, simulating the extraction of the strip specimen from the pipe. At this step, residual stresses are reduced to zero but the plastic deformations due to the forming process are maintained. Finally, a second step is performed with the "unit cube" model applying (a) uniaxial compression in the hoop direction of the pipe and (b) uniaxial tension in the direction parallel to the pipe axis, representing the loads (external pressure and bending, respectively) during pipe installation.

Figure 12 depicts stress-strain compressive response in hoop direction at the intrados and the extrados of the pipe. Figure 13 illustrates the axial tensile stress-strain response and the hoop compressive stress-strain response. The results show that the compressive yield stress in the hoop direction (420MPa) is lower than the corresponding tensile yield stress in the longitudinal direction (480MPa) of the pipe; both values are calculated on the basis of a 0.2% residual strain and are significantly different than the initial yield stress of the steel plate material equal to 498MPa.

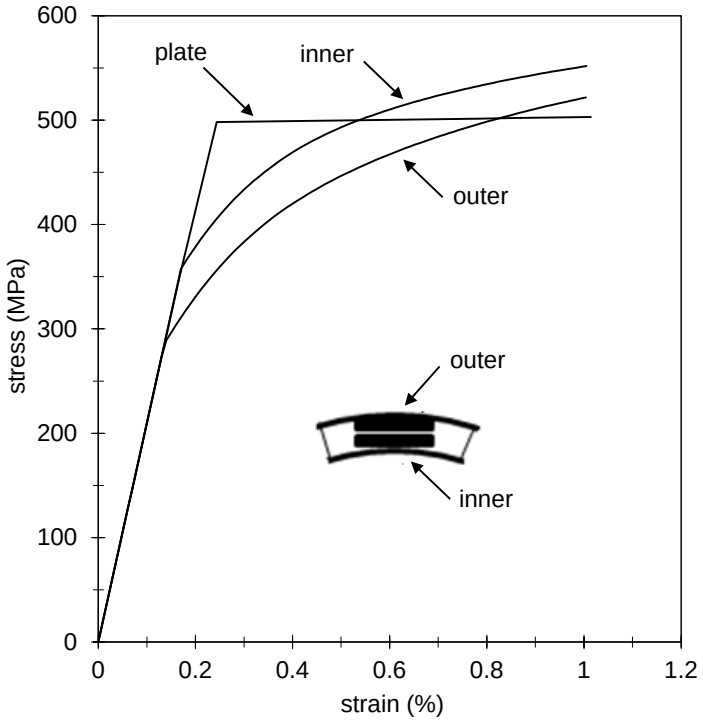

Figure 12: Compression hoop stress-strain response of pipe at "intrados" and "extrados"; non-homogeneity of mechanical properties across the thickness of the pipe.

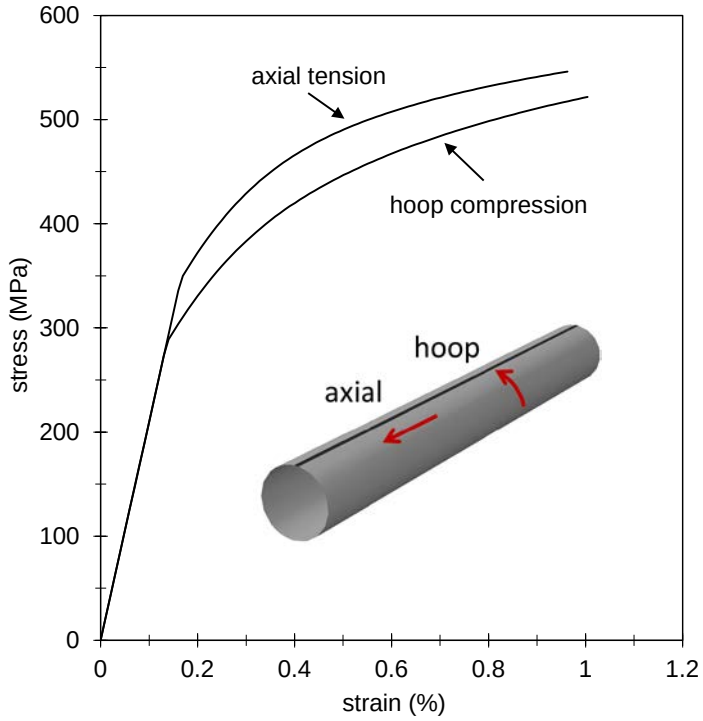

Figure 13: Axial tensile and hoop compression stress-strain response of JCO-E; anisotropy of the mechanical properties in the axial and hoop direction.

4 NUMERICAL SIMULATION OF THE STRUCTURAL BEHAVIOR OF JCO-E PIPES

Following the simulation of the forming process, the JCO-E pipe under consideration at the last stage of the analysis procedure is subjected to external pressure, so that the pressure ultimate capacity is determined.

Each of the forming parameters of the JCO-E manufacturing process has an important effect on the response of JCO-E pipes under external pressure. The effect of thermal load during welding and the effect of the two different geometries of the weld part on the ultimate pressure are presented for the case of 9 punching steps through a short parametric analysis. Figure 14 compares the ultimate collapse pressure obtained from the analysis as described in section 2, and an analysis in which no thermal load is applied to the weld part, referred as "mechanical analysis". The maximum difference on the ultimate pressure value is computed equal to 0.6MPa (i.e. less than 2%) indicating that the cold bending process is primarily responsible for the mechanical response under external pressure. In addition, Figure 15 shows that the choice of the weld part geometry may not be significant for the ultimate pressure capacity.

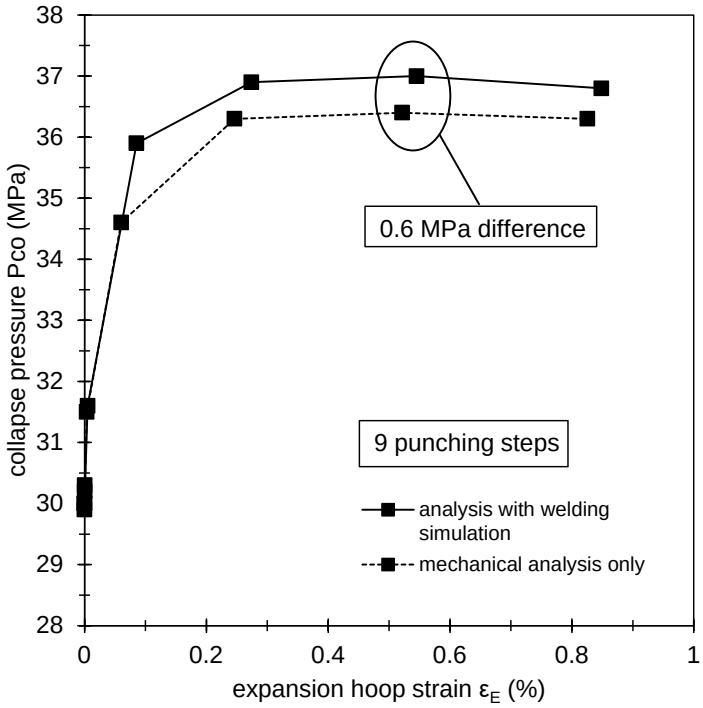

Figure 14: Ultimate capacity of JCO-E pipes under external pressure for different values of expansion hoop strain; (a) using the present analysis that includes thermomechanical simulation of welding process, (b) using a purely mechanical model that accounts only for the forming process.

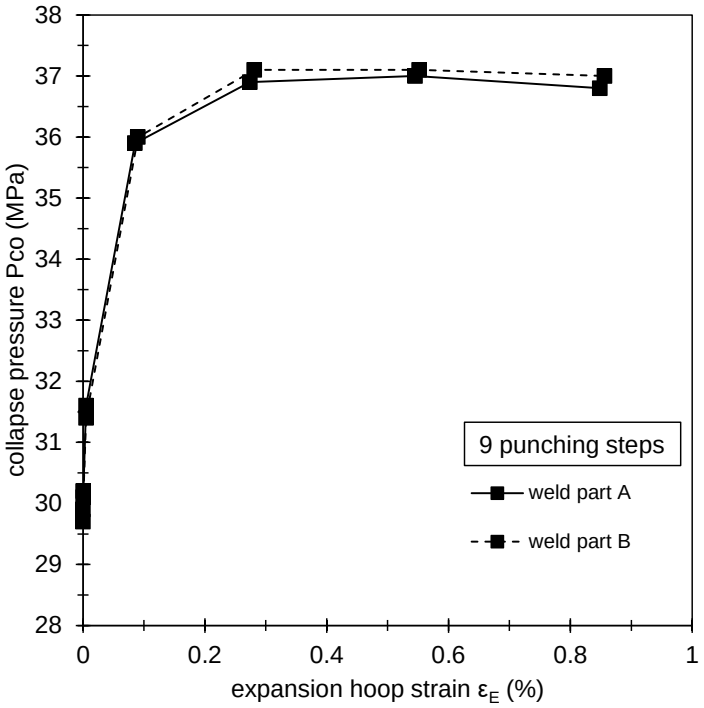

Figure 15: Collapse pressure of JCO-E pipe under external pressure for different values of expansion hoop strain for the two different configurations of the weld part.

The effects of expansion (i.e. the value of ε_E) and the number of punching steps on the ultimate external pressure of the pipe are also examined through a numerical analysis. In Figure 16, the predicted collapse pressure of the pipe, denoted as P_{CO}, for the three cases of punching step number under consideration, is presented with respect to the applied expansion hoop strain ε_E. It is important to note that, starting from the JCO case $(\varepsilon_E = 0\%)$, initial ovality drops sharply with increasing values of ε_E for the cases of 9 and 19 punching steps as noted in Figure 9, resulting to the increase of P_{CO}, shown in Figure 16. For the case of 15 punching steps the initial ovality slightly reduces as expansion hoop strain increases, so that the collapse pressure increases. On the other hand, relatively small values of ovalization correspond to large values of the expansion hoop strain, which are associated with significant residual stresses induced by the cold-forming process, resulting to a decrease of the maximum collapse pressure. More specifically, this is attributed to the reduction of the compressive strength of the material due to Bauschinger effect. In other words, the Bauschinger effect appears to counteract the beneficial effects of expansion. The numerical results (Figure 16), show that a maximum value of P_{CO} is reached for each case under consideration, at a value of ε_E equal to 0.54% (9 punching steps), 0.41% (15 punching steps) and 0.25% (19 punching steps) respectively. Further increase of ε_E reduces the value of collapse pressure. Therefore, there exists an optimum expansion at which highest resistance against external pressure instability (buckling) is achieved, an observation which is consistent with the results reported in [10]. It is worth mentioning that the pipe with 15 punching steps is capable of sustaining higher values of external pressure than the case with 9 and 19 punching steps. This is an indication that 15 punching steps could be the optimum number of punching

steps to deform the plate to a pipe. Application of more punches leads to overlapping of the deformed areas due to each punch. On the other hand, if less steps are used, the ovality of the pipe is lower than the other two cases, and results in lower pressure resistance. Figure 17 shows the response of pressurized pipes in terms of a pressure-ovalization diagram for the three different cases at optimum expansion level. Figure 18 depicts the deformed JCO-E pipe at maximum pressure, at two post-buckling stages corresponding to Δ equal to 9.1% and 17.2%, for the case of 9 punching steps and zero expansion (ε_E = 0% , "JCO" case). The above numerical results are in agreement with the relevant conclusions reported in [11].

Furthermore, a comparison between a JCO-E and a seamless pipe with the same geometric and material characteristics subjected to external pressure is examined. Seamless pipes have negligible residual stresses at the end of their manufacturing process. Herein, the seamless pipe is considered stress free, and initial ovalization has been imposed in the original geometry of the numerical model. In Figure 19 the results of a seamless pipe and JCO-E pipe with 9 punching steps are depicted. The seamless pipe can sustain higher pressure than the corresponding JCO-E pipe with the same ovalization. This difference ranges from approximately 50% for small initial ovality values (large expansion) to 30% for higher ovality (small expansion).

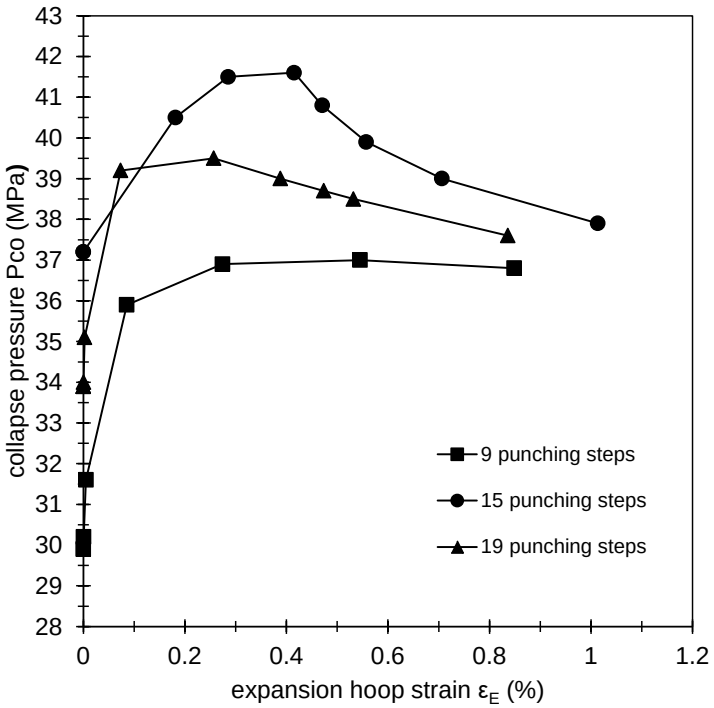

Figure 16: Variation of collapse pressure of JCO-E pipes in terms of expansion hoop strain, for the three cases of punching steps.

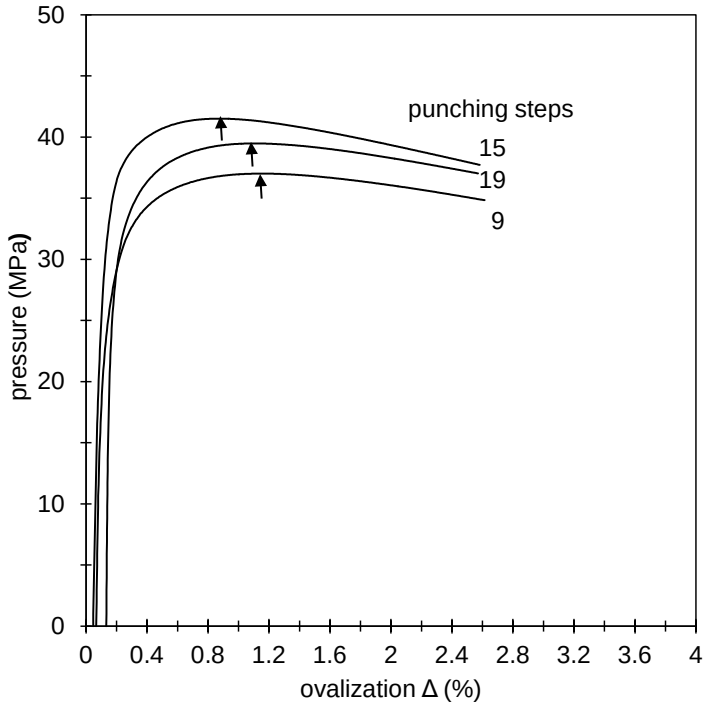

Figure 17: Calculated pressure-ovalization response of JCO-E pipes subjected to external pressure, considering the optimum expansion hoop strain for each case.

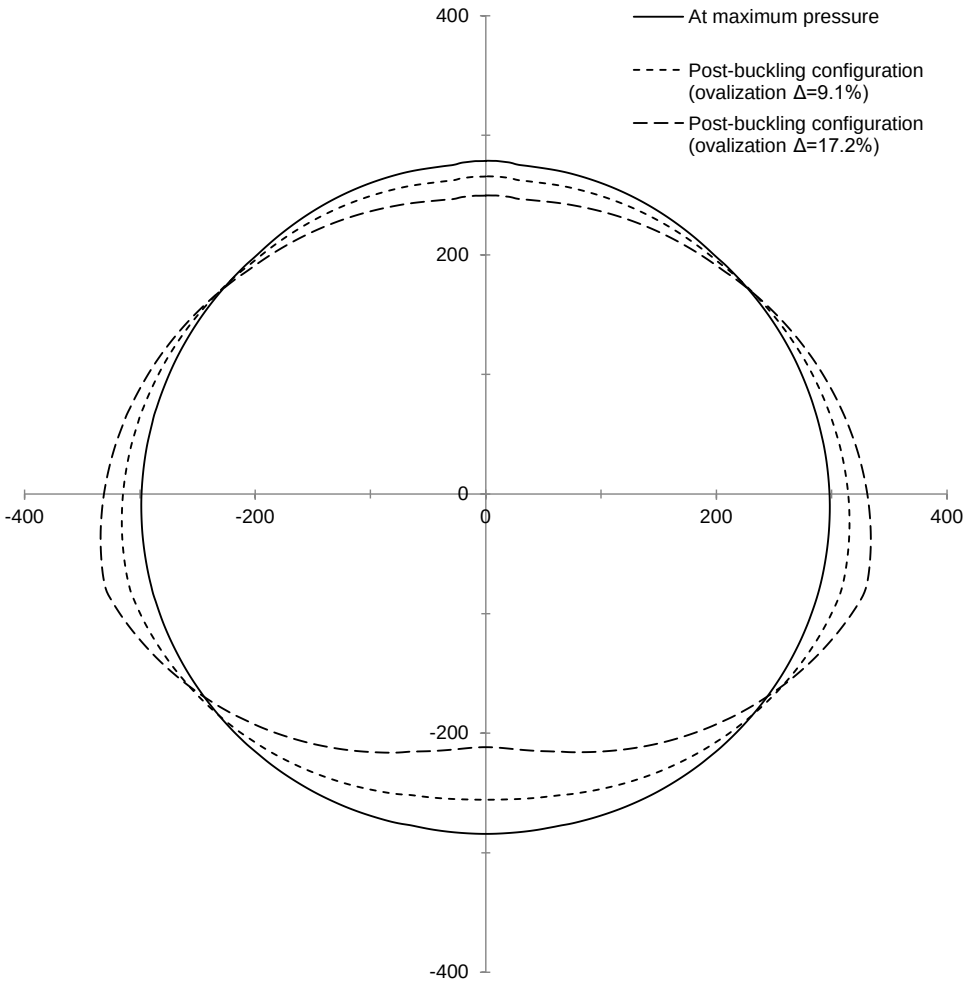

(a)

Post-buckling configuration (ovalization Δ=17.2%)

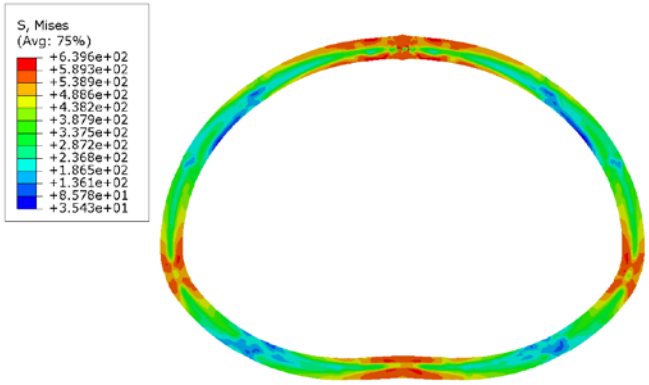

(b)

Figure 18: Deformed configuration of the pipe under external pressure for the case of 9 punching steps and zero expansion (JCO case); (a) cross-sectional shape at three stages of deformation; (b) distribution of von Mises stress and cross-sectional configuration at post-buckling stage corresponding to ovalization Δ=17.2%.

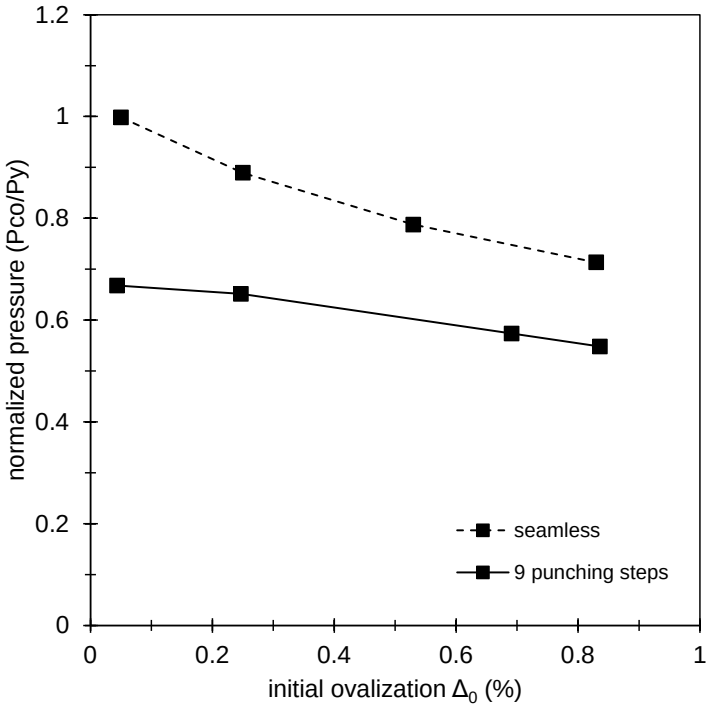

Figure 19: The effect of initial ovalization on the collapse pressure of 9 punching steps JCO-E and comparison with the collapse pressure of an equivalent seamless pipe.

5 CONCLUSIONS

The present paper presents a rigorous simulation of the JCO-E manufacturing process and its effect on the mechanical behavior of offshore pipes, subjected to external pressure. The simulation uses advanced finite element simulation tools, capable at describing the entire deformation history from the initial plate configuration to the post-buckling configuration of the pipe in a sequence of interrelated analysis steps. Furthermore, the analysis includes the simulation of welding process through an appropriate thermo-mechanical analysis. A plasticity model that describes the important features of nonlinear elastic–plastic material behavior is employed within the finite element model, using a material user subroutine. In the first part of the paper, the JCO-E cold-bending manufacturing process stages and the welding process are simulated in detail, considering a 24-inch-diameter (609.6mm) pipe, with a nominal thickness equal to 32.33mm (1.273 in) focusing on the effects of manufacturing process on material properties. The yield stress of the line pipe material is somewhat lower than the initial yield stress of the steel plate, which is mainly attributed to the forming process. A slight reduction of the initial plate thickness with respect to the thickness of the JCO-E pipe is also noted due to the cold forming process. In the second part of the paper, a numerical analysis is conducted on the effects of manufacturing process on the overall pipe behavior against pressure. The numerical results show that increase of expansion hoop strain leads to minimization of pipe out-of-roundness and, up to a certain limit value of expansion, it is beneficial for the ultimate pressure capacity of the pipe. Beyond this limit value of expansion, the collapse pressure resistance of the pipe is reduced due to the Bauschinger effect, so that there exists an optimum expansion at which highest resistance against external pressure loading can be achieved. Furthermore, the effect of thermal

loading seems to be negligible for the external pressure capacity of the pipe. As a result, it is important to be mentioned that the numerical tools developed in the present study can be employed for optimizing the JCO-E manufacturing process in terms of pressure capacity.

REFERENCES

[1] Kyriakides, S., Corona, E., 2007. *Mechanics of offshore pipelines*, Buckling and Collapse, Vol. 1, Elsevier.

[2] Kyriakides, S., Corona, E., Fischer, F. J., 1991. "On the Effect of the UOE Manufacturing Process on the Collapse Pressure of Long Tubes", *Offshore Technology Conference* Vol. 4, OTC 6758, pp. 531–543. Also, published in *Journal Engineering for Industry*, Vol. 116, pp. 93–100.

[3] Gresnigt, A.M., Van Foeken, R.J., Chen, S., 2000. "Collapse of UOE Manufactured Steel Pipes", *Proceedings of the Tenth International Offshore and Polar Engineering Conference*, Vol. 2. pp. 170-181, Seattle, Washington.

[4] DeGeer, D., and Cheng, J.J., 2000. "Predicting Pipeline Collapse Resistance", *International Pipeline Conference*, Alberta, Canada.

[5] Herynk, M.D., Kyriakides, S., Onoufriou, A., Yun, H.D., 2007. "Effects of the UOE/UOC Pipe Manufacturing Processes on Pipe Collapse Pressure", *International Journal of Mechanical Sciences*, Vol. 49, pp. 533–553.

[6] Chatzopoulou, G., Karamanos, S. A., Varelis, G. E., 2016. "Finite Element Analysis of UOE Manufacturing Process and its Effect on Mechanical Behavior of Offshore Pipes", *International Journal Solids and Structures*, Vol. 83, pp. 13–27.

[7] Toscano, R. G., Raffo, J., Mantovano, L., Fritz, M., Silva, R. C., 2007. "On the Influence of the UOE Process on Collapse and Collapse Propagation Pressure of Steel Deep-Water Pipelines under External Pressure", *Offshore Technology Conference*, Houston, Texas.

[8] Chandel, J. D., Singh, N. L., 2011."Formation of X-120 M Line Pipe through J-C-O-E Technique", *Engineering*, Vol. 3, pp. 400-410.

[9] Gao, Y., Li, Q., Xiao, L., 2009. "Numerical Simulation of JCO/JCOE Pipe Forming", *World Congress on Computer Science and Information Engineering*, Los Angeles, CA, USA.

[10] Krishnan, V.R., Baker, D.A., 2014. "Enhanced Collapse Resistance of Compressed Steel Pipes". *Proceedings of the 33rd International Conference on Ocean, Offshore and Arctic Engineering*, San Francisco, California, USA.

[11] Reichel, T., Pavlyk, V., Beissel, J., Kyriakides, S., Jang, W.Y., 2011. “New Impander Technology for Improved Collapse Resistance of Large Diameter Pipe for Deepwater Applications”, *Offshore Technology Conference*, Houston, Texas.

[12] Yan, C., Liu, C., Zhang, G., 2014. "Simulation of Hydrogen Diffusion in Welded Joint of X80 Pipeline Steel", *J. Central South University*, Vol. 21, pp. 4432-4437.

[13] Horn, T., 2003. "Cyclic Plastic Deformation and Welding Simulation", *Doctoral Thesis*, Faculty of Materials Science, Delft University of Technology Press.

[14] Yaghi, A. H., Tanner, D. W. J., Hyde, T. H., Becker, A. A., Sun, W., 2012. "Finite element thermal analysis of the fusion welding of a P92 steel pipe", *Mechanical Sciences*, Vol. 3, pp. 33-42.